Characterisation of the wind-driven halo in 5 years of VLT/SPHERE-IRDIS data

Félix Sauvourel
Supervised by F. Cantalloube
June 2026

High-contrast imaging (HCI)

8-m class telescopes

Adaptive Optics (AO)

Coronagraph

Post-processing

High-contrast imaging (HCI)

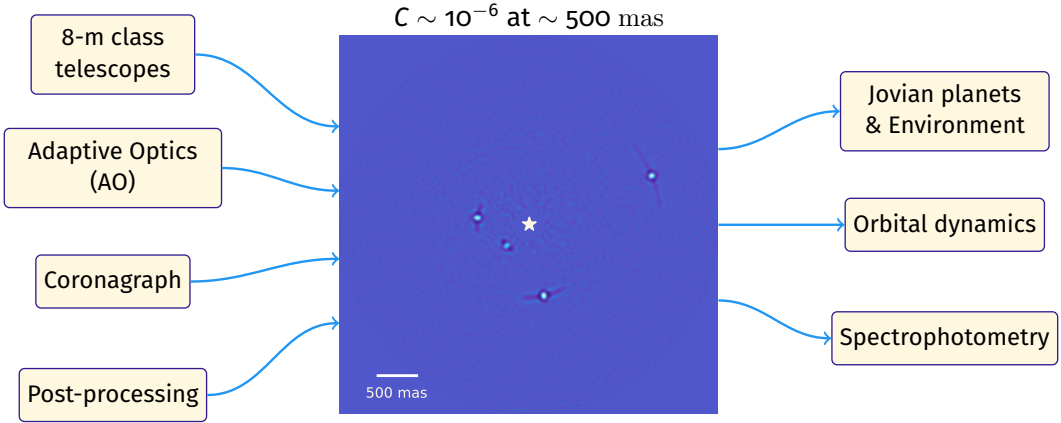

HR 8799 Marois et al. (2008)

Digging the contrast

Exoplanet imaging:

- Current facilities: $C \sim 10^{-6}$
  $\rightarrow$ Young giant gaseous planets
- Bright residuals (AO, non-common path aberrations) are well understood

Reach fainter errors $\Rightarrow$ **Wind-Driven Halo**

Digging the contrast

Exoplanet imaging:

- Current facilities: $C \sim 10^{-6}$
  $\rightarrow$ Young giant gaseous planets
- Bright residuals (AO, non-common path aberrations) are well understood

Reach fainter errors $\Rightarrow$ **Wind-Driven Halo**

Wind-driven halo (WDH)

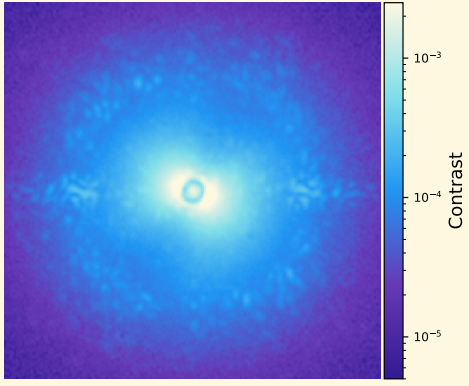

$C_{\text{without}} \sim 10^{-4}$ Vs $C_{\text{WDH}} \sim 10^{-3}$

Strong frame variations

$\sim$ 30% acquisitions

Wind-driven halo (WDH)

Servolag-error

$$\sigma^2_{\text{servo}} = (\tau_{\text{AO}}/\tau_{\text{o}})^{5/3}$$

Coherence time

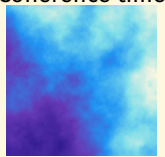

Vs

AO loop delay

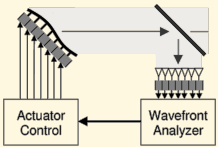

- $\tau_{\text{o}} \propto r_{\text{o}}/v_{\text{eff}}$
- $\tau_{\text{AO}} \rightarrow t_{\text{int}} \rightarrow V_{\text{mag}}$

Wind-driven halo (WDH)

Servolag-error

$$\sigma^2_{\text{servo}} = (\tau_{\text{AO}}/\tau_0)^{5/3}$$

Coherence time

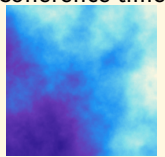

Vs

AO loop delay

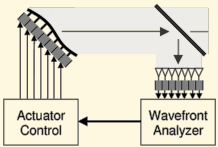

- $\tau_0 \propto r_0/v_{\text{eff}}$
- $\tau_{\text{AO}} \rightarrow t_{\text{int}} \rightarrow V_{\text{mag}}$

Parametrization

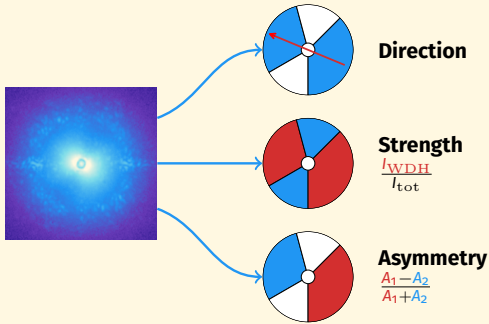

Wind-driven halo (WDH)

Servolag-error

$$\sigma^2_{\text{servo}} = (\tau_{\text{AO}}/\tau_0)^{5/3}$$

Coherence time

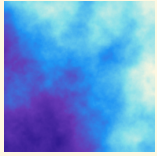

Vs

AO loop delay

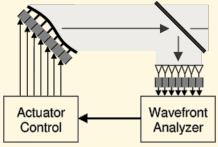

- $\tau_0 \propto r_0/v_{\text{eff}}$
- $\tau_{\text{AO}} \rightarrow t_{\text{int}} \rightarrow V_{\text{mag}}$

Parametrization

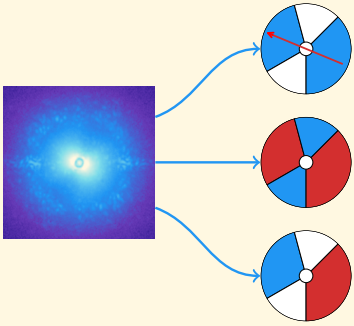

Goal: Characterize the WDH w/ archives

- Scheduling
- Post-processing optimization
- AO Control

SPHERE Archives

SPHERE-IRDIS H-band: SHINE GTO
789 observations/74k frames

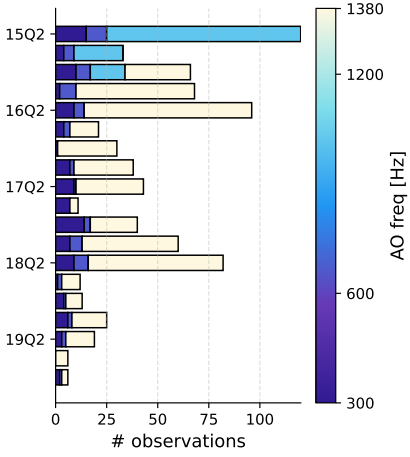

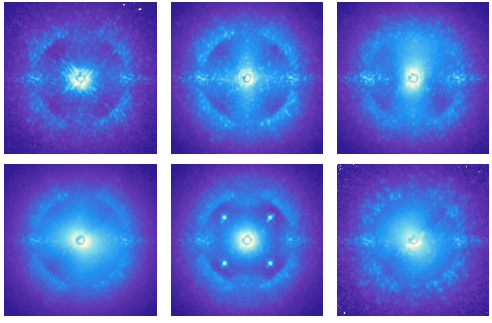

Very diverse images
⇒ **Need for a robust WDH characterization pipeline**

WDH characterization Pipeline

Raw cube

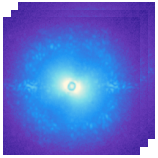

WDH characterization Pipeline

Raw cube

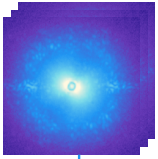

Mask &
low-pass

WDH characterization Pipeline

Raw cube

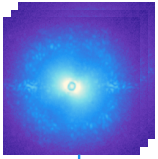

Mask & low-pass

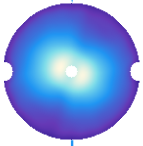

Polar prof. & fit

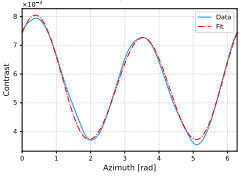

WDH characterization Pipeline

Raw cube

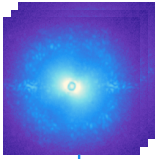

Mask & low-pass

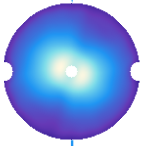

Polar prof. & fit

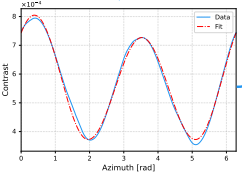

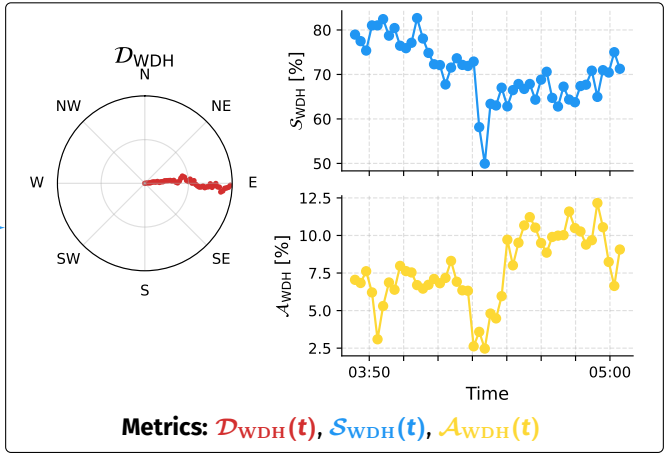

WDH proxy

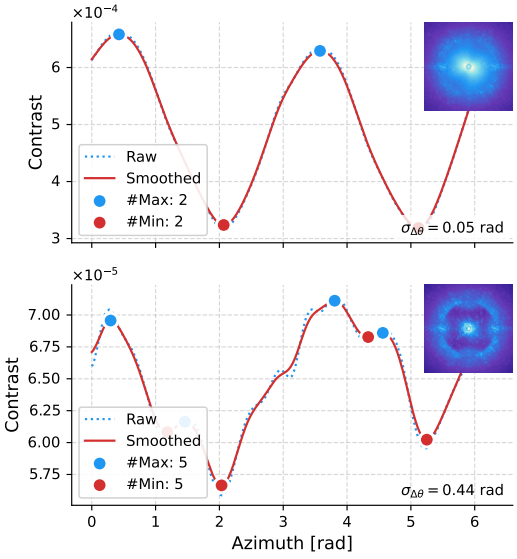

Proxy signature of WDH

Based on WDH geometry:

- 2 minima & 2 maxima
- Regular separation of $\frac{\pi}{2} \rightarrow \sigma_{\Delta\theta} \sim 0$

Increased robustness

- Slice away from center and outer edge
- Gaussian smoothing

$\Rightarrow$ validation with simulations
work in progress

WDH occurence rate 1/2

WDH angular proxy: threshold to classify **WDH** vs **no WDH**
Visual inspection of random sampling of 100 cubes → ROC curve to find the optimal threshold

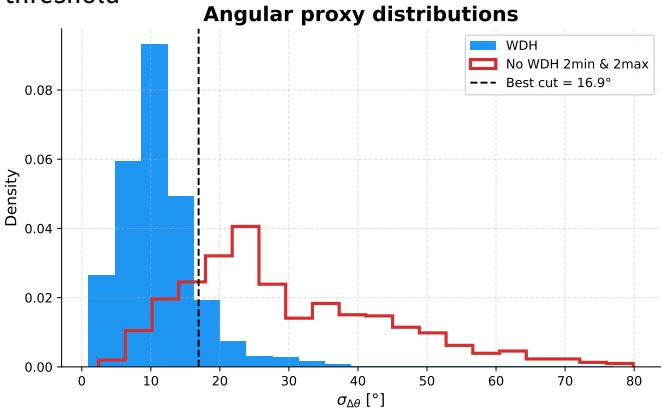

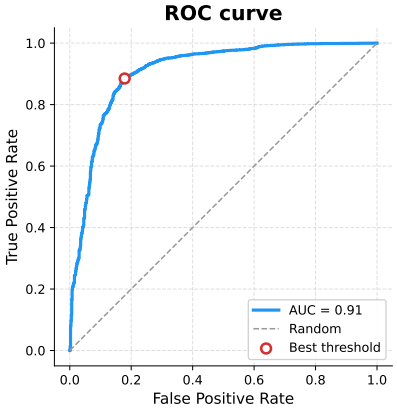

⇒ **WDH criteria**: 2 minima & 2 maxima & $\sigma_{\Delta\theta} < 16.9°$

WDH occurence rate 2/2

Apply criteria to the full GTO sample

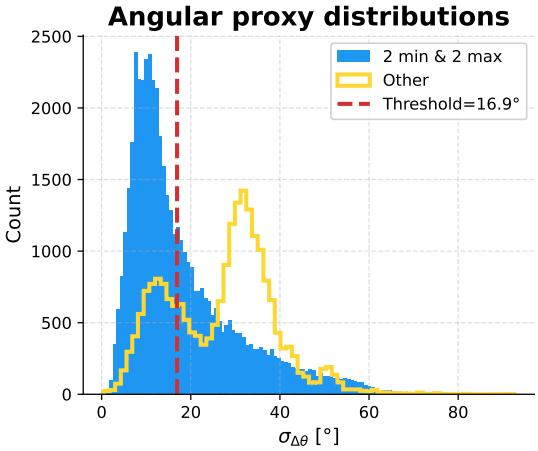

⇒ **WDH occurence rate:** $\sim$ 33%

- Seems conservative (random sample occurence rate $\sim$ 70%)
- But in accordance with previous studies (Cantalloube et al., 2020)

AO Freq	300	600	1200	1380
WDH Occ.	75%	47%	38%	23%

WDH occurence rate 2/2

Apply criteria to the full GTO sample

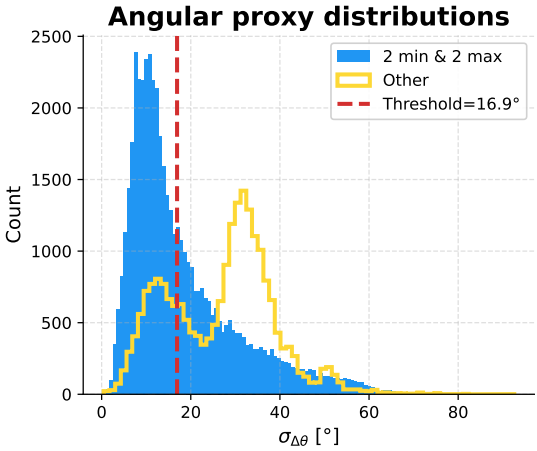

⇒ **WDH occurence rate:** ∼ 33%

- Seems conservative (random sample occurence rate ∼ 70%)
- But in accordance with previous studies (Cantalloube et al., 2020)

AO Freq	300	600	1200	1380
WDH Occ.	75%	47%	38%	23%

Origin

Correlations with:

- AO telemetry
- In situ meteorological data
- Reanalysis meteorological data

Jet stream importance 1/3

Key finding of Cantalloube et al. (2018), Madurowicz et al. (2018): WDH is correlated with the jet stream

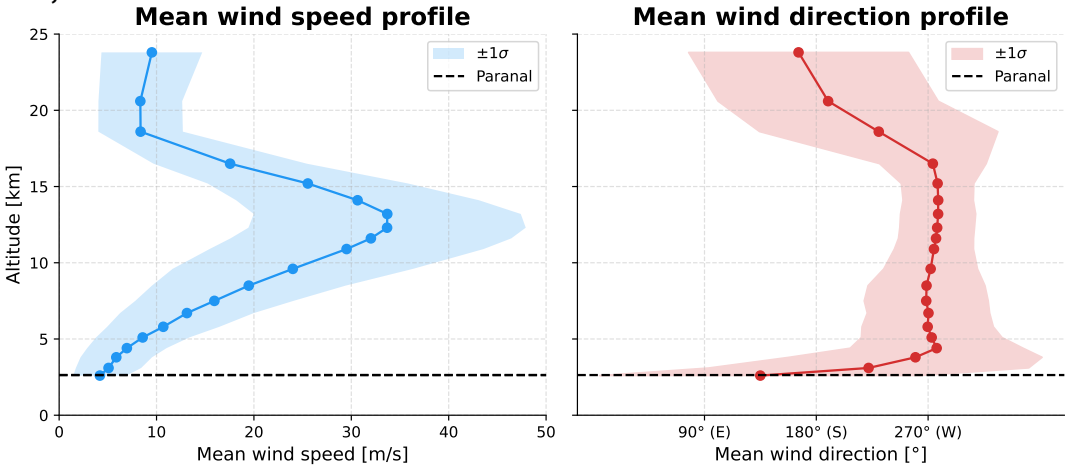

Jet stream importance 2/3

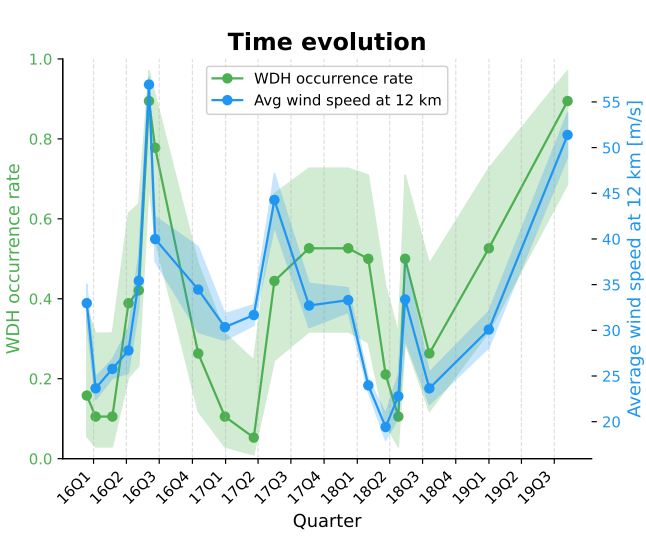

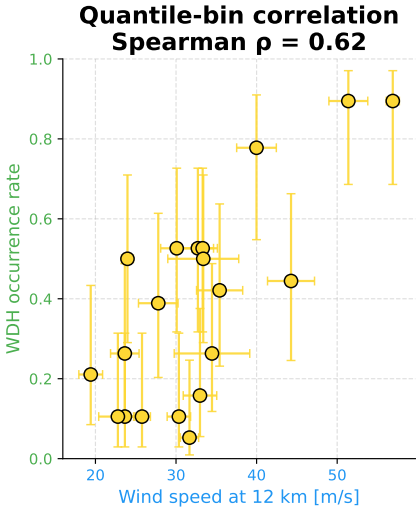

Jet stream importance 3/3

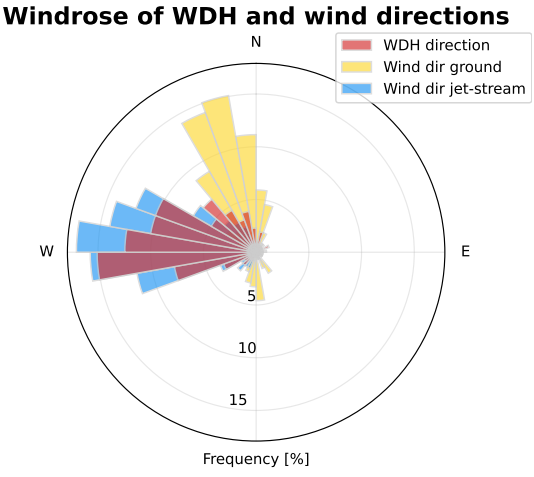

Jet stream importance 3/3

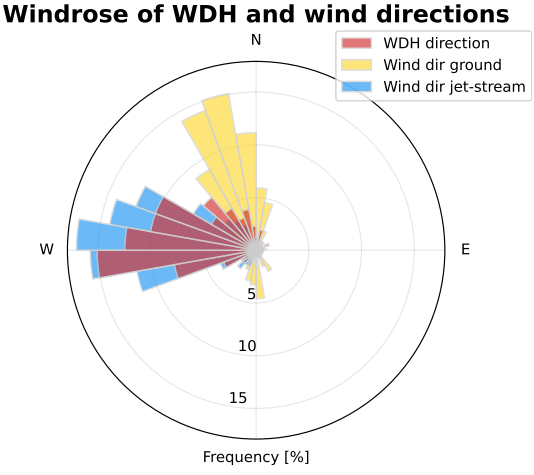

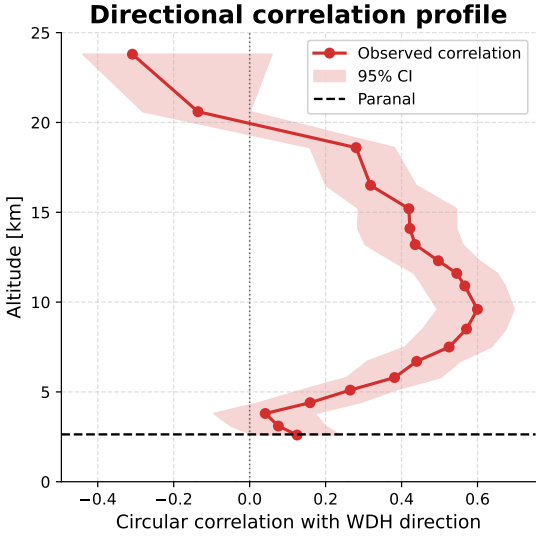

WDH strength & turbulence coherence time

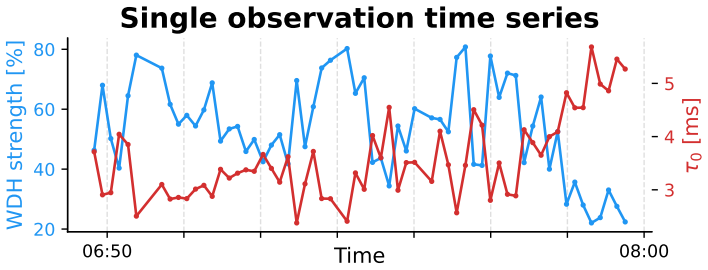

WDH strength & turbulence coherence time

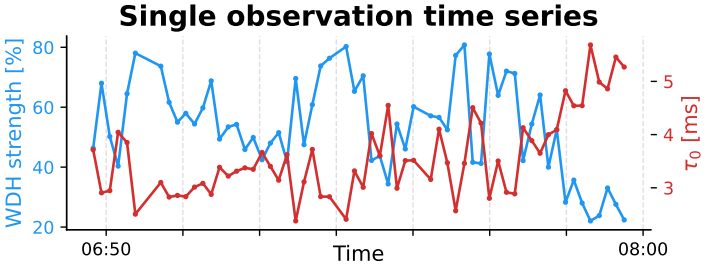

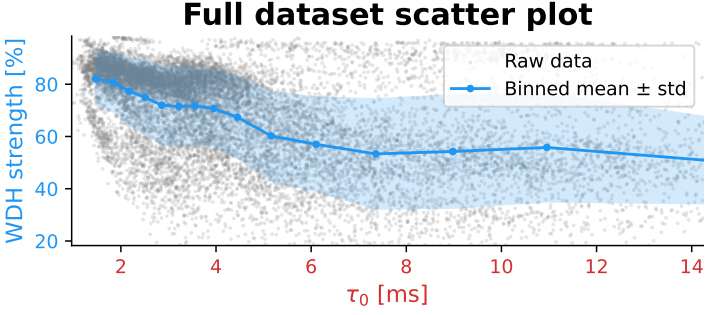

WDH strength & turbulence coherence time

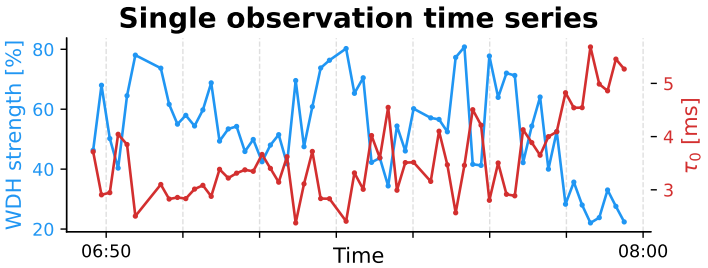

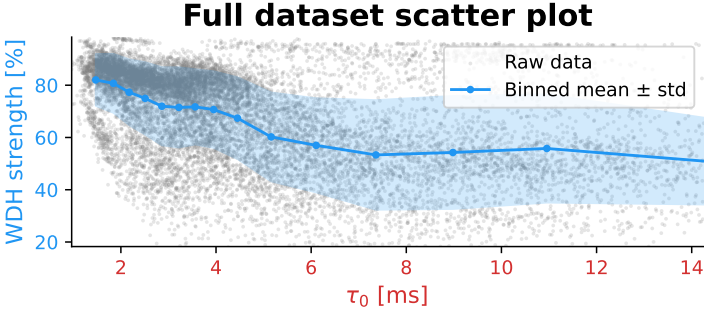

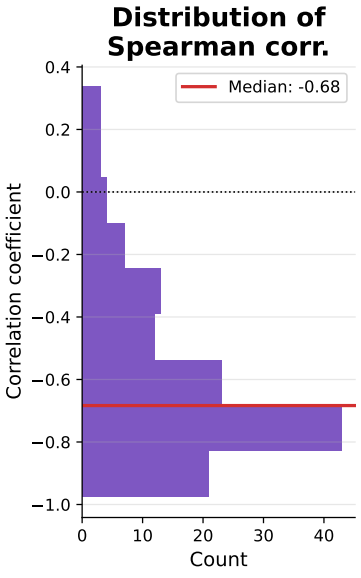

Takeaways

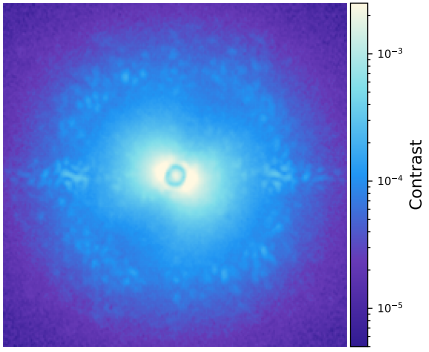

Work done

- Robust characterization pipeline on GTO-Hband
- WDH occ. rate $\sim$ 33%
- Jet stream led WDH

Potential usages

- Scheduling
- Post-processing optimization
- AO control optimization

Next

- Validation on simulations *HCIPy* Por et al. (2018)
- Correlate other metrics
- Extend the analysis

Takeaways

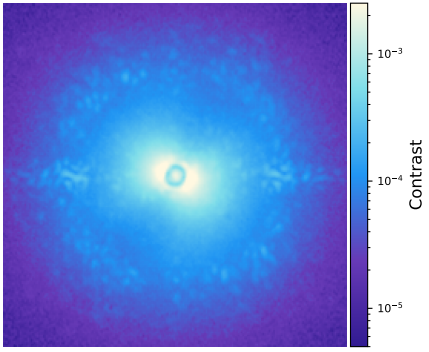

Work done

- Robust characterization pipeline on GTO-Hband
- WDH occ. rate $\sim$ 33%
- Jet stream led WDH

Potential usages

- Scheduling
- Post-processing optimization
- AO control optimization

Next

- Validation on simulations *HCIPy* Por et al. (2018)
- Correlate other metrics
- Extend the analysis

Large HCI dataset $\rightarrow$ what else could we explore ?

Bibliography i

F. Cantalloube, E. H. Por, K. Dohlen, J.-F. Sauvage, A. Vigan, M. Kasper, N. Bharmal, T. Henning, W. Brandner, J. Milli, C. Correia, and T. Fusco. Origin of the asymmetry of the wind driven halo observed in high-contrast images. *Astronomy & Astrophysics*, 620:L10, Dec. 2018. ISSN 1432-0746. doi: 10.1051/0004-6361/201834311. URL http://dx.doi.org/10.1051/0004-6361/201834311.

F. Cantalloube, O. J. D. Farley, J. Milli, N. Bharmal, W. Brandner, C. Correia, K. Dohlen, T. Henning, J. Osborn, E. Por, M. Suárez Valles, and A. Vigan. Wind-driven halo in high-contrast images: I. analysis of the focal-plane images of sphere. *Astronomy & Astrophysics*, 638:A98, June 2020. ISSN 1432-0746. doi: 10.1051/0004-6361/201937397. URL http://dx.doi.org/10.1051/0004-6361/201937397.

A. Madurowicz, B. A. Macintosh, J.-B. Ruffio, J. Chilcote, V. P. Bailey, L. A. Poyneer, E. Nielsen, and A. P. Norton. Characterization of lemniscate atmospheric aberrations in gemini planet imager data. In D. Schmidt, L. Schreiber, and L. M. Close, editors, *Adaptive Optics Systems VI*, page 230. SPIE, July 2018. doi: 10.1117/12.2314267. URL http://dx.doi.org/10.1117/12.2314267.

C. Marois, B. Macintosh, T. Barman, B. Zuckerman, I. Song, J. Patience, D. Lafreniere, and R. Doyon. Direct imaging of multiple planets orbiting the star hr 8799. *Science*, 322(5906):1348–1352, Nov. 2008. ISSN 1095-9203. doi: 10.1126/science.1166585. URL http://dx.doi.org/10.1126/science.1166585.

Bibliography ii

E. H. Por, S. Y. Haffert, V. M. Radhakrishnan, D. S. Doelman, M. van Kooten, and S. Bos. High contrast imaging for python (hcipy): an open-source adaptive optics and coronagraph simulator. In D. Schmidt, L. Schreiber, and L. M. Close, editors, *Adaptive Optics Systems VI*, page 152. SPIE, 2018. doi: 10.1117/12.2314407. URL http://dx.doi.org/10.1117/12.2314407.

Dépendances physique des paramètres du WDH

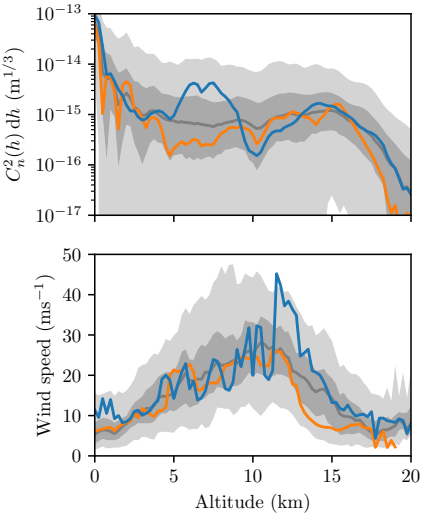

Cantalloube et al. (2020, 2018)

- vitesse de vent effective

$$v_{\text{eff}} = \left(\frac{\int_0^{+\infty} C_n^2(z) v(z)^{5/3} dz}{\int_0^{+\infty} C_n^2(z) v(z) dz} \right)^{3/5}$$

- Paramètre de Fried $r_0 \propto \lambda^{5/6}$
- Temps de cohérence de l'atmosphère $\tau_0 = 0.314 \frac{r_0}{v_{\text{eff}}}$
- Direction du WDH suit celle du vent effectif
- Force du WDH $\propto v_{\text{eff}}, \lambda^{-2}, \Delta t_{\text{OA}}$
- Asymétrie du WDH $\propto \frac{zf\lambda}{v_{\text{eff}} \Delta t_{\text{OA}}}$